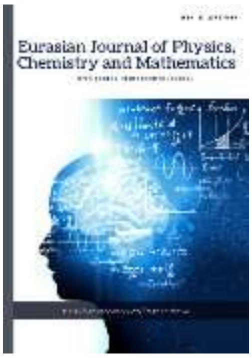

The Effect of Substituents on the Properties of Porphyrin and metalloprophyrin Semiconductors Using Density Functional Theory

Ashraq T. Atwan[1]
[1*] Physics Department, Science College, Thi-Qar University, Nassiriya – Iraq.
ashraq522@gmail.com

Mohammed L. Jabbar [2]
[2]Physics Department, Science College, Thi-Qar University, Nassiriya – Iraq.

ABSTRACT

A few porphyrins and their metal complex (metalloporphyrin) assume huge parts in detecting, photodynamic treatment, attractive reverberation imaging (MRI), anticancer medications, electronic gadgets, and fluorescence imaging. In this work, the impact of changing the focal metal was thought about, as titanium metal and cadmium metal were utilized. As well as adding chlorine atom to the focal metal, as well as concentrating on the impacts of various closures of the compound, once by making hydrogen at the meso-closes and again by making phenyl rings at the meso-closes. Furthermore, information on all past impacts on electronic properties and their improvement. For instance, the energy of filled and HOMO and LUMO, the energy gap, hardness, delicate quality compound electronegativity, and electrophilicity are determined. It very well may be seen that the chose materials have a lower energy gap than the pure porphyrin. The energy gap of the mixtures examined, which are all situated in the semiconducting locale (1.109352 - 2.91692 eV), can thusly be utilized in significant electronic applications like sensors, transistors and solar cells. All computations were done with the Gaussian 09 programming package.

Keywords: Porphyrin; Density Functional Theory; Energy Gap; Metals; Infrared Spectra.

1. Introduction

In last years, porphyrin have demonstrated their financial plausibility in the production and improvement of most electronic gadgets and the chance of involving them in electronic gadgets present and in the future[1,2]. A porphyrin is a major ring atom comprised of four pyrroles[1,3], which are more modest rings comprising of four carbons and one nitrogen. These pyrrole atoms are connected by an arrangement of single and twofold bonds. framing a tremendous ring. A tetra-pyrrole is the specialized name for four pyrroles connected together[4–9]. The ring has an extremely even dissemination of electrons around its distance across. Accordingly, a porphyrin is a compound. A porphyrin compound. is very steady in this state. Porphin is the model of a nonexclusive porphyrin[10]. This particle is just experienced as halfway in nature very sometimes, yet it is the groundwork of all porphyrin compound. . The last examination in porphyrin is one-layer (two dimensions) compounds (i.e., the rings are level in space) or three-dimensional[11], in which there are many investigations at the degree of hypothetical research[7,12–16] and viable research[17–20] to comprehend and acquire actual properties that can be applied in electronic advances. Metalloporphyrins have been utilized as strong impetuses in a wide scope of substance processes[8,21–25]. detecting, photodynamic treatment (PDT), attractive reverberation imaging (MRI),anticancer drugs, electronic gadgets, and fluorescence imaging in light of their particular specific endorsement and maintenance[5,26].

The electronic design properties of the ground condition of the metalloporphyrin were done in hypothetical way by involving the first principle in the hypothesis DFT calculations. The main principle. The upsides of HOMO and LUMO energies, energy values, Fermi level ionization potential, electronegativity(χ), electrophilicity (ω), and electrostatic potential were considered, as well as gathering electronic properties, bringing about IR spectra.

2. Computational Details

Porphyrin is a natural compound. It is basically made out of four pyrrole rings associated with one another by inclining spans in a shut style to frame an enormous ring toward the end. It is the easiest tetrapyrrole compound, which is a strong, sweet-smelling compound[5]. Current hypothetical estimations have been explored using the primary guideline calculation in the thickness practical hypothesis (DFT)[27–29]). Though the calculation improvement was accomplished utilizing the B3LYP model[30]. These images allude to Becke's three boundaries. Lee-Yang-Parr additionally is known as the cross breed functional [31–33]. which is viewed as a great decision to research the streamlining in the illumination of DFT. The 6-31G premise set was utilized quantum substance computation [34,35]. All systems could be relaxed before energy investigations for porphyrin and metalloporphyrin (porphyrin with metals of both Titanium (Ti) and Cadmium (Cd) atoms). This process is termed "geometry optimization." The electronic properties of porphyrin include the energy of the Fermi level, the highest occupied molecular orbital (HOMO) energies, the lowest unoccupied molecular orbital (LUMO) energies, and energy gaps (the difference between the eigenvalues of the maximum valence band and the minimum conduction band or by mathematically speaking expressed[27,36–38]

$$E_g = E_{LUMO} - E_{HOMO} \qquad (1)$$

Structures are studied theoretically with involve of Ti and Cd impurities.

According to Koopman's approximation in which the frontier orbital energies are given by the following relationship[29,39,40]

$$I.P. = -HOMO \; E.A. = \; -LUMO \,\} \qquad (2)$$

Subsequently, the ionization potential (I.P) and electron affinity (E.A) values can be used to determine electronegativity, hardness, softness, and electrophilicity.

Mulliken electronegativity (χ) is an index that describes the tendency or power of a functional group or an atom in a structure to attract electrons[38,40].

$$\chi = \frac{I.P + E.A}{2} \qquad (3)$$

The global hardness was proposed by Parr and Pearson define

$$\eta = \frac{1}{2}\left(\frac{\partial^2 E}{\partial N^2}\right)_V \qquad (4)$$

After simplifying the equation 4 can be rewritten as

$$\eta = \frac{I.P - E.A}{2} \qquad (5)$$

Also, global softness is defined by the reverse of hardness by the following relationship

$$\sigma = \frac{1}{2\eta} \qquad (6)$$

The electrophilicity index is defined as

$$\omega = \frac{\chi^2}{2\eta} = \frac{(I.P + E.A)^2}{4(I.P - E.A)} \qquad (7)$$

Finally, the Fermi level can be written as

$$F_L = \frac{E_{HOMO} + E_{LUMO}}{2} \qquad (8)$$

3. Results and Discussion

3.1 Geometry optimization

In the first stage, the shape of porphyrin was designed, including 20 carbon atoms, 4 nitrogen atoms and 14 hydrogen atoms. The carbon atoms are built as rings of a quad lattice. The structure of porphyrin treated with hydrogen passivation decreases the boundary effects. Subsequently, the structure is treated until it reaches the best position for stability. This process is called geometry optimization. However, we did not observe the apparent deformation of pristine porphyrin and their directions. The preceding certainly agrees with figure 1.

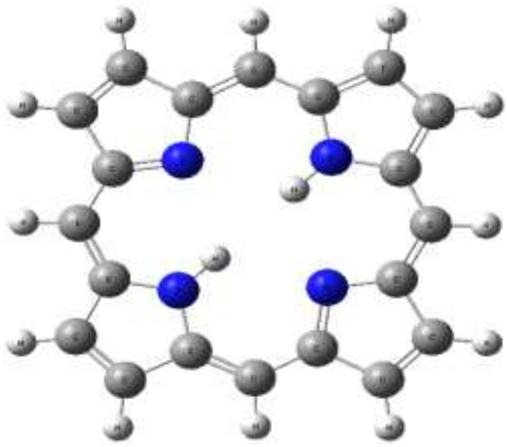

Figure 1. Geometry optimization of pure porphyrin

The second stage is the addition of some impurities to the pristine porphyrin to get a new enhanced property such as electronic, optical, mechanical, and several properties. The pristine structure is doped by Titanium (Ti) and Cadmium (Cd) atoms. All these structures are clearly shown in figure 2, which involves Double Titanium meso-tetra (4-hydrogen) porphyrin (DTiTHP),Double Cadmium meso-tetra(4-hydrogen) porphyrin(DCdTHP),Titanium meso-tetra (4-carboxyphenyl) porphyrin(TiTCPP), Titanium-Chlore meso-tetra (4-carboxylphenyl) porphyrin (TiClTCPP), Cadmium meso-tetra(4-carboxyphenyl)porphyrin (CdTCPP), Cadmium-Chlore meso-tetra(4-carboxyphenyl) porphyrin (CdClTCPP), Cadmium-Chlore meso-tetra(4-hydogen) porphyrin (CdClTHP). It is important to visualize that the simulation for all the structures is performed using the DFT method with the B3LYP hybrid functional in the light of the Gaussian 09 software package. [41] Eventually, the vibrational spectrum is calculated without imaginary wavenumbers. This result confirms that the structures deduced correspond to minimum energy.

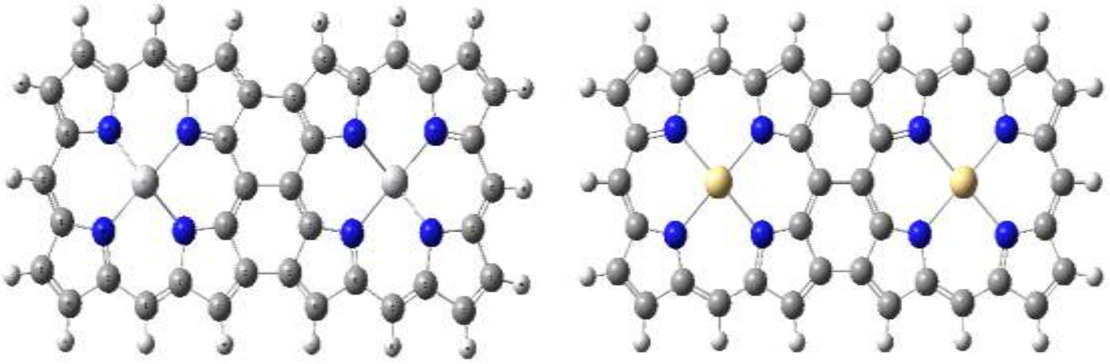

DTiTHP

DCdTHP

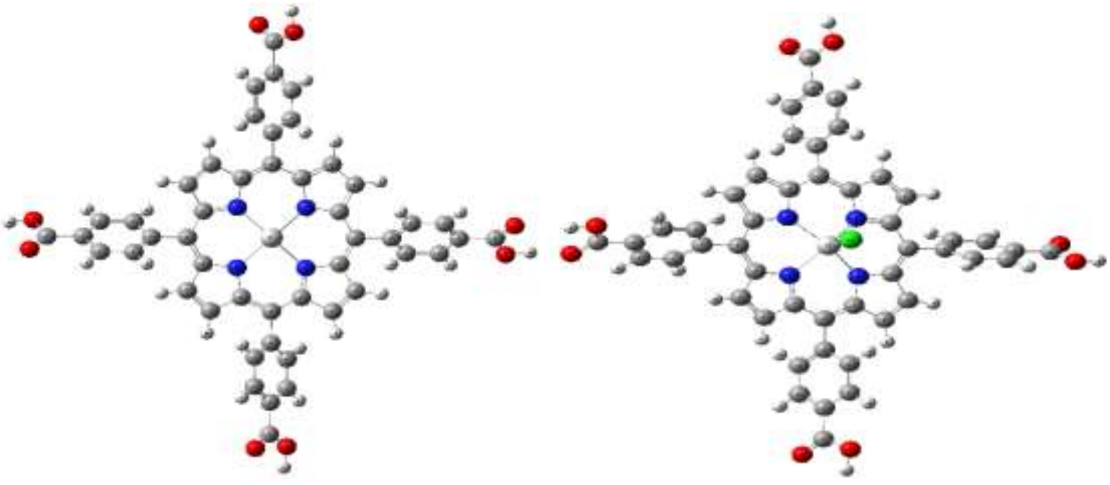

TiTCPP TiClTCPP

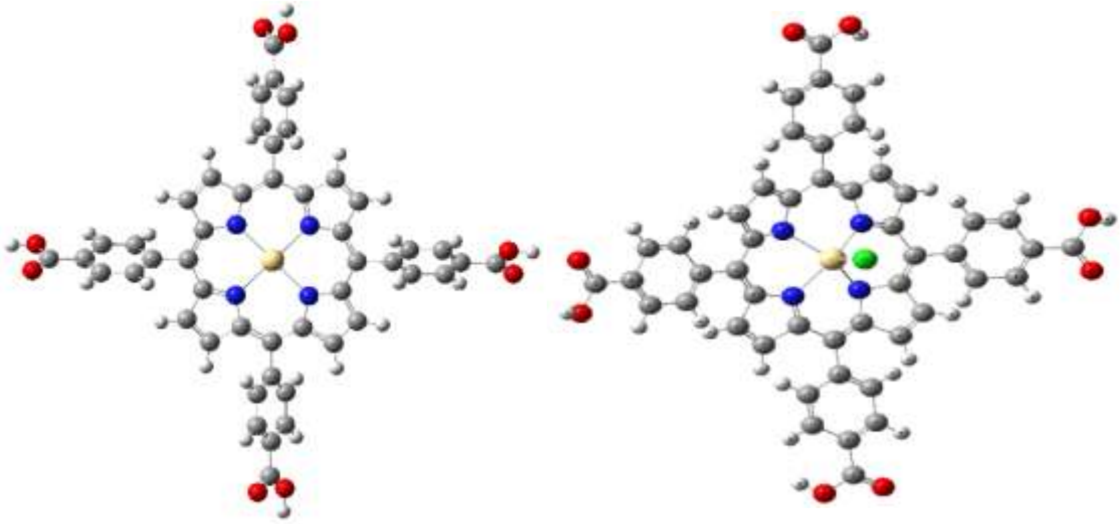

CdTCPP CdClTCPP

Figure 2: geometry optimization of metalloporphyrin in different sites where Ti, Cd, and Cl represent Titanium, Cadmium, and chlorine atoms, respectively.

3.2 Infrared spectra

There are two kinds of stretching oscillations: symmetric and asymmetrical. When similar atoms stretch in the same direction, this is referred to as symmetric stretching.

When they oscillate in the same phase, asymmetric stretching is happening when the bonds oscillate in a variety of phases. Infrared spectra yield harmonics of vibrational frequencies. Low frequencies give torsion vibrations.

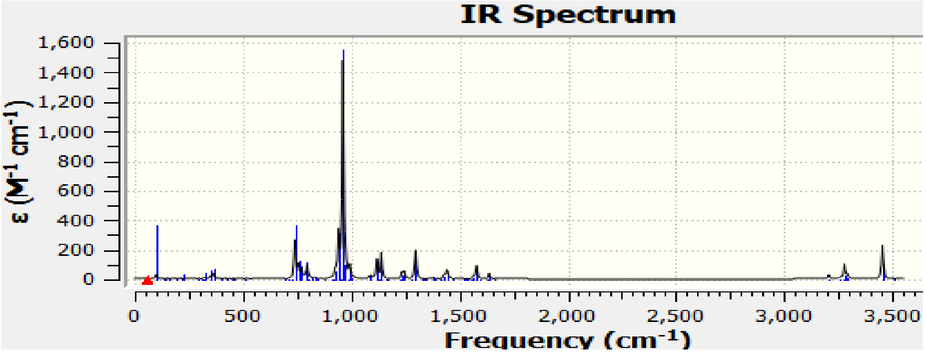

DCdTH

Porphyrin

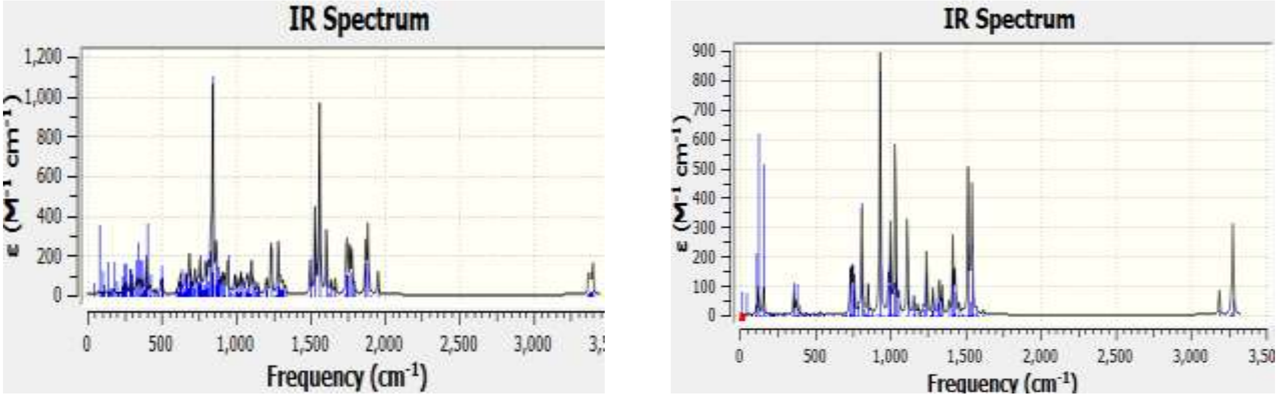

DTiTHP P

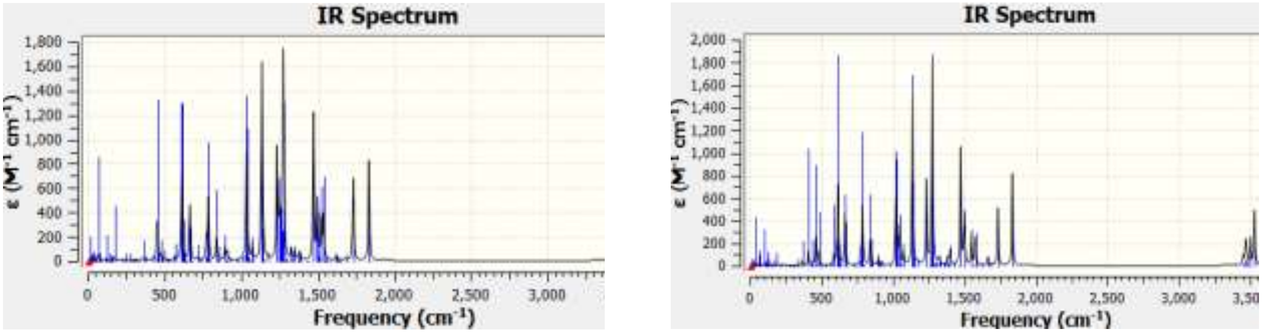

TiTCPP TiClTCPP

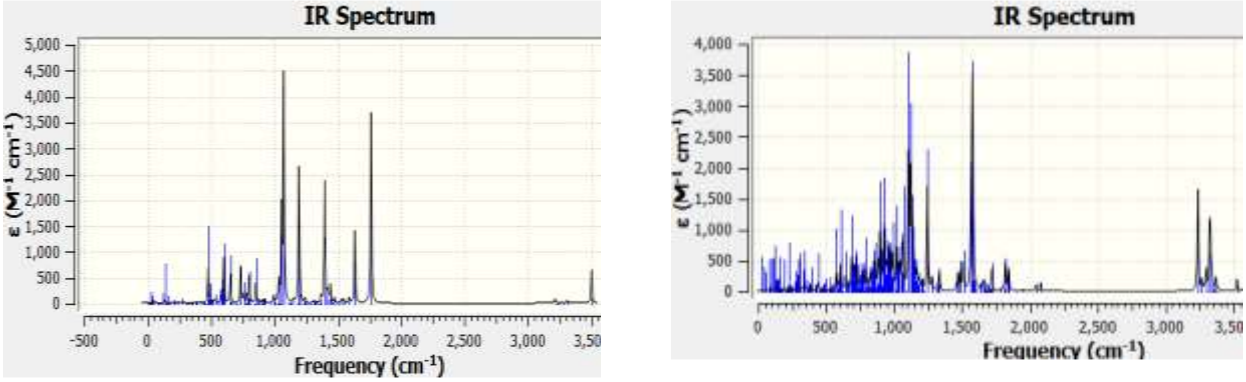

CdTCPP CdClTCPP

Figure3. the infrared spectra of all structure such as porphyrin and metalloporphyrin (metals are Ti, Cd)

Figure 3 elucidates that there are other pinnacles. Each pinnacle represents a bond between two neighboring particles, whereas the results are in good agreement with experimental data[2,5]. All charts of the infrared spectra have peaks between 650-1000 cm^{-1}, these peaks are attributed to the vibrations and absorption of carbon atoms with double bonds. Moreover, it contains peaks with a frequency of 1640 cm^{-1}, which results from the vibration of bonds between carbon and nitrogen atoms. The other peaks represent the presence of other impurity atoms such as metals (Ti, Cd) and chlorine atoms.

3.3 Contours

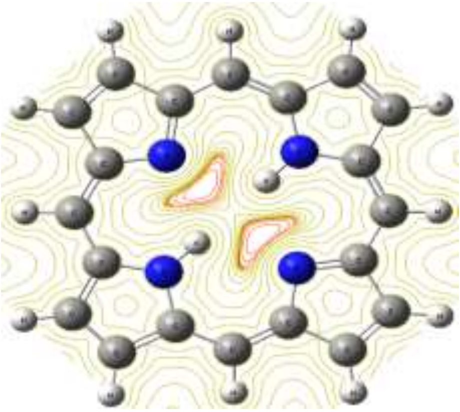

Porphyrin

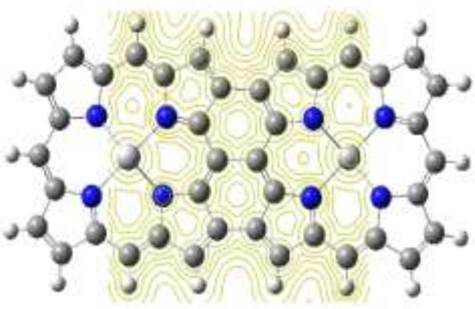

DTiHP

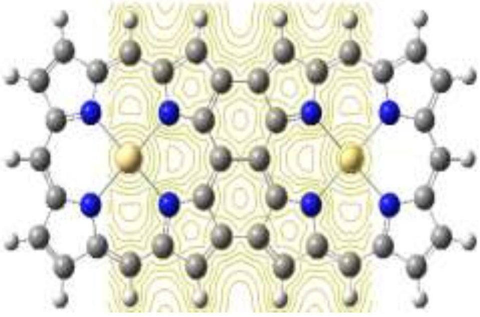

DCdHP

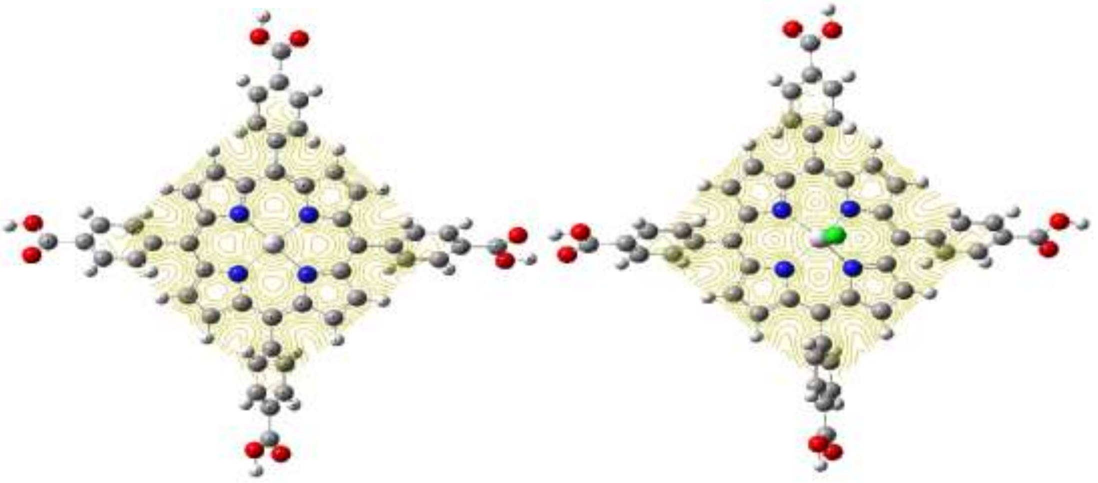

TiTCPP

TiClTCPP

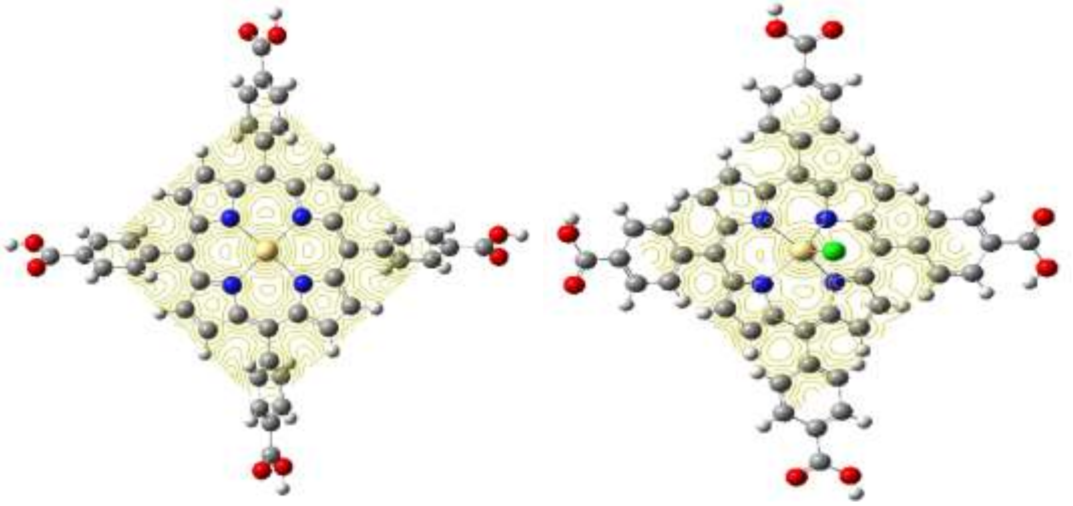

CdTCPP

CdClTCPP

Figure 4. Electrostatic potential (ESP) contour map of porphyrin and metalloporphyrins, respectively

That the pure compound porphyrin has a distortion in the distribution of negative charges, so it appears in red in the center of the compound, while the rest of the compounds, that is, after adding the metal to the porphyrin (metalloporphyrin), are more stable and the distribution of the charge is more uniform, so the Berillion zones are on the The shape of semi-regular circles is not significantly distorted. This may be attributed to the amount of positive and negative charges present in the compound, in addition to their density of distribution in the compound. Finally, the central circle is between the carbon atoms. These circles represent the regions of Brillion, where the first central circle represents the zone of the first Brillion. And the second circle represents the second Brillion zone, and so on with the other bands. Naturally, the electrons in the first region cannot move to the region of the second Brillion, except when there is more energy than the energy of the region forbidden between them.

3.4 Density of states (DOS)

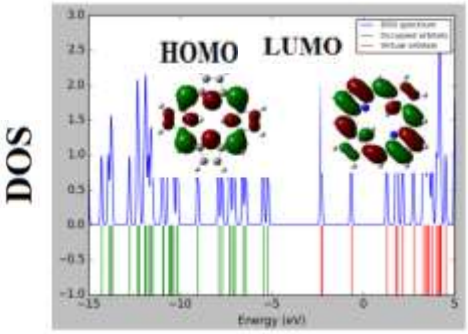

porphyrin

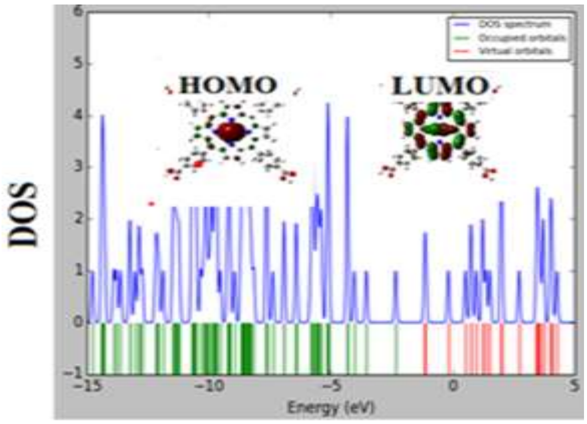

DTiHP

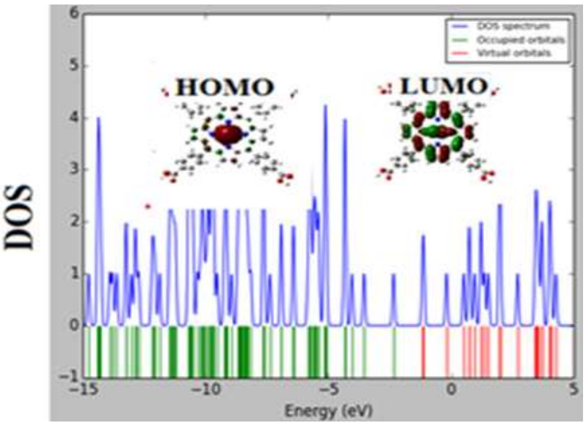

DCdHP

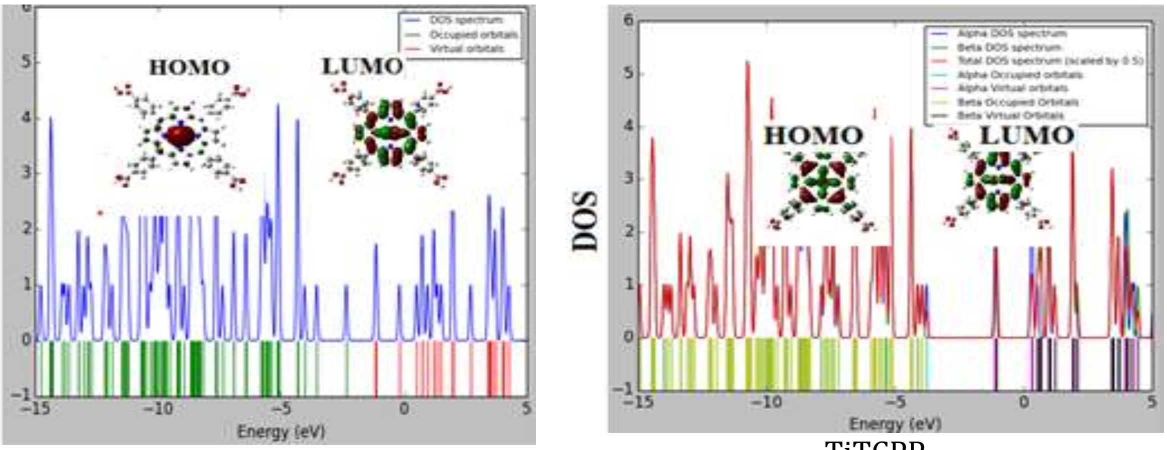

TiClTCPP TiTCPP

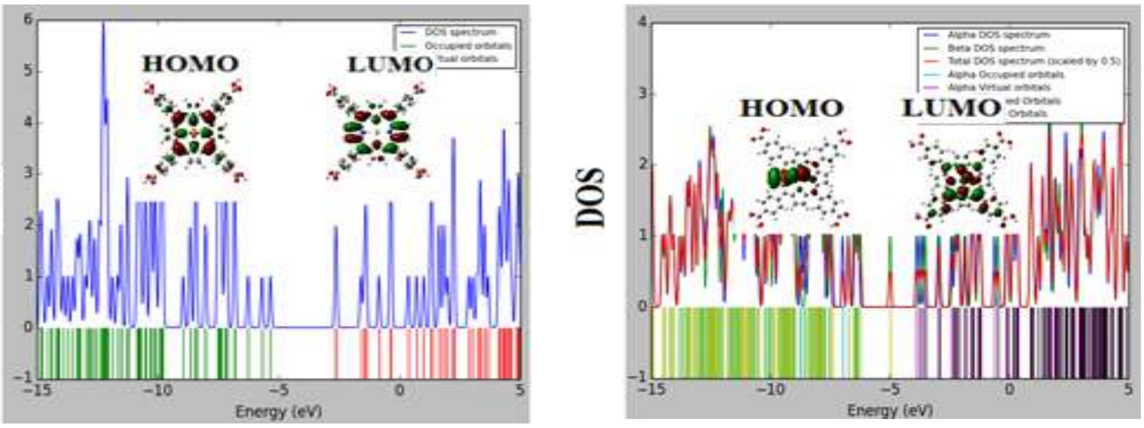

CdTCPP CdClTCPP

Figure (5) DOS and both diagrams of HOMO and LUMO for pure Porphyrin and metalloporphyrin (metals are Ti, Cd

The linear interference between atomic orbitals can give molecular orbitals. Thus, molecular orbitals can produce both the HOMO and LUMO surfaces. The above figures can show that both HOMO and LUMO regions have new colors. There are two interpretations of these colors as following The first explanation includes the positive part of the wave function can be indicated by green color, while the negative part of the wave function is indicated by the dark red color.

The second explanation involves the positive part of the electrostatic potential zone is indicated by the green color while the negative part of the electrostatic potential zone is indicated by a dark red color.

Anyone can notice the difference between the HOMO and LUMO forms with and without impurities. For example, the dissimilarity between the HOMO and LUMO surfaces of a pure

Porphyrin structure versus the HOMO and LUMO surfaces can be clearly noticed after the addition of impurities such as Titanium (Ti) and Cadmium (Cd). This difference in the surface shape can be attributed to the effect of the interaction between the original structure of Porphyrin and the added atoms. For example; Current surfaces have been performed for pure Porphyrin and metalloporphyrin with doping by using density functional theory in Gaussian 09 package. In general, the density of state increases with increasing the electron energy. Thus, there are many available states being occupied at a certain energy level with a high density of state. On the other hand, there are not available energy level being occupied at the DOS,equals to zero[44]

3.5 Electronic Properties

This section refer to the electronic properties physical such as the values of HOMO,LUMO, band gap, ionization potential (I.P), electron affinity (E.A), electronegativity (χ), and electrophilicity (ω), softness (σ) , hardness (η), and Fermi level energy.

Table (1) shows the frontiers energies and energy gap (Eg)

SYSTEM	LUMO (eV)	HOMO (eV)	Eg (eV)
Porphyrin (P)	-2.2842	-5.20119	2.91692
DTiTHP	-2.54141	-3.86491	1.323494
DCdTHP	-3.17187	-4.85018	1.678313
TiTCPP	-1.15534	-2.34196	1.186628
TiClTCPP	-1.11126	-0.377267	2.66141
CdTCPP	-2.6206	-5.33153	2.710932
CdClTCPP	-3.86763	-6.31816	2.450533

Table 1 represents the values of the lowest empty level within the conduction beam and the highest filled level within the valence beam. Energy gap values were also calculated using equation No. 1. The results of the energy gap appear in Table 1. In fact, the energy gap value obtained for porphyrin agrees well with the results[45]. When comparing the energy gap values for porphyrin before and after doping, it can be noted that the energy gap values for all compounds became lower, which is a good result. It is also clear that the value of the energy gap when adding titanium metal to porphyrin is less than the value of the energy gap when adding cadmium metal to porphyrin. This is an important result because all the energy gap values are located in the semiconductor region. . It is also important to mention that the obtained energy gap values are very useful, especially in electronic applications such as solar cells and sensors. For example, the value of the energy gap of the compound porphyrin with titanium(TiTCP) is similar to the value of the energy gap of silicon.

Table(2)the values of ionization potential (I.P), electron affinity (E.A), electronegativity (χ), and electrophilicity (ω).

Compound	I.P(eV)	E.A(eV)	X(eV)	ω(eV)
Porphyrin (P)	5.20119	2.2842	3.864364	4.80213
DTiTHP	3.864908	2.541414	3.203161	3.394843
DCdTHP	4.850183	3.17187	4.011026	6.750313
TiTCPP	2.341965	1.155337	1.748651	0.907112
TiClTCPP	3.772667	1.111256	2.441961	3.967614
CdTCPP	5.331527	2.620595	3.976061	10.71432
CdClTCPP	6.318162	3.867629	5.092896	15.89023

Table 2, all values are calculated by using the expression in equations (2, 3, and 7 In fact, the ionization potential and electron affinity are crucial because they can be used to forecast chemical bond strength. They can also be utilized as indicators of whether an atom or molecule will become an electron donor or acceptor. They depend on the type of metal and geometry structure sequent their values become larger or smaller by compare with the value of pure porphyrin. They can also be utilized as indicators of whether an atom or molecule will become an electron donor or acceptor. They depend on the type of metal and geometry structure, so their values become larger or smaller by comparing them with the value of pure porphyrin as shown in table 2. For example, the largest value of I.P and E.A after adding impurities at the electron I.P. of Cadmium chlorine meso-tetra(4 carboxylphenyl) porphyrin (CdClTCP) is (6.318162) eV, and the structure of CdClTCP has an E.A of (3.867629)eV. On the other hand, the structure with the smallest values of I.P and E.A to the (TiTCP) structure has I.P (2.341965)eV) and the structure has E.A(1.155337)eV). Furthermore, both I.P. and E.A. are represented as primary bases to predict and obtain other properties. So, it can be used as a sensor device.

The value of the electronegativity for the structure CdClTCP is higher and equal to) 5.092896)eV. This means that these structures have a stronger ability to attract the shared electrons. The values of the electrophilicity fluctuate up and down compared to the value of the pristine compound (porphyrin without metal). The reason for changing electrophilicity values is the geometric structure, type, and position of impurities according to the acidity or basicity of Lewis. The values of the electrophilicity fluctuate up and down compared to the value of the porphyrin. Systems doped with porphyrin- (Ti and Cd) have the highest electronegativity values.

Table(3)the values of, softness (σ) , hardness (η), and Fermi level enrg

Compound	σ(eV)	η(eV)	F.L(eV)
Porphyrin (P)	0.342819	1.46417	-3.86436
DTiTHP	0.330874	0.661747	-3.20316
DCdTHP	0.419578	0.839156	-4.01103
TiTCPP	0.296657	0.593314	-1.74865
TiClTCPP	0.665353	1.330705	-2.44196
CdTCPP	0.677733	1.355466	-3.97606
CdClTCPP	0.612633	1.225266	-5.0929

Depending on previous equations and Table 3, we can see that the energy gap is a function of the chemical hardness. When the structure has a higher value of hardness, it means the structure has a large energy gap. For instance, the porphyrin structure has values for the hardness and energy gap (at ground state), which are equal to (1.46417 eV). Softness is equal to the inverse of the hardness, which leads to the largest value of hardness corresponding to the smallest value of softness, for example, 0.342819 eV and vice versa. In harvesting, hardness and softness are parameters that are very important because they can be used to test both the performance and sensitivity of explosive molecules.

It is clear that the Fermi level values of metalloporphrin compounds change. These changes in values in comparison with the original porphyrin can be attributed to the crystal structure and the type of metal used. As shown in table 3, For example, the Fermi level values for all structures are lower than the location of the Fermi level for pure porphyrin (-4.02694 eV). Also, one can notice that the lowest value of the Fermi level is for the compound CdClTCP, at (-5.0929)eV

4. Conclusions

In this work, the electronic properties of porphyrin and metalloporphyrin were achieved theoretically by using DFT algorithms, the B3LYP technique, and 6-311G (d, p). No imaginary frequency values appeared in the results obtained for all compounds, which means that the results are correct and accurate. Three crucial characteristics must be combined: the first, appropriate structural porphyrin features; the second, an adequate central metal; and the third, suitable metalloporphyrin. Regarding the choice of the central metal, when using a phynol ring and hydrogen, Ti (IVB) and Cd (IIB) are widely accepted as the most suitable central metals. From the metalloporphyrin structure, we can conclude that the best compounds are those that contain titanium atoms in meso-carboxylate rings and Double meso-hydrogen porphyrin (viz: TiTCP and DTiTHP). It is important to mention; compounds containing a chlorine atom exhibit ferromagnetic behavior. The energy gaps in these structures are the smallest. This result is an important ground state energy gap for all metalloporphyrin compounds located in the semiconducting region, and this gives designers and manufacturers freedom to choose the material and use it in electronic applications. The hardness values of the metalloporphyrin materials are greater than the softness values, which indicates that these compounds are stable.

Acknowledgments

The authors express their appreciation to the PC and Knowledge Networking Center at Thi-Qar University/College of Science for the assistance in facilities for high-performance computing.

Conflicts of Interest:

The authors declare no conflicts of interest.

References

[1] S. Hiroto, Y. Miyake, H. Shinokubo, Synthesis and functionalization of porphyrins through organometallic methodologies, Chem. Rev. 117 (2017) 2910–3043.

[2] D.R. Roy, E. V Shah, S.M. Roy, Optical activity of Co-porphyrin in the light of IR and Raman spectroscopy: a critical DFT investigation, Spectrochim. Acta Part A Mol. Biomol. Spectrosc. 190 (2018) 121–128.

[3] F. Bryden, R.W. Boyle, Metalloporphyrins for medical imaging applications, in: Adv. Inorg. Chem., Elsevier, 2016: pp. 141–221.

[4] Y. Kabe, M. Ohmori, K. Shinouchi, Y. Tsuboi, S. Hirao, M. Azuma, H. Watanabe, I. Okura, H. Handa, Porphyrin accumulation in mitochondria is mediated by 2-oxoglutarate carrier, J. Biol. Chem. 281 (2006) 31729–31735.

[5] M.E. Önal, MOLECULAR MAGNETIC MATERIALS BASED ON PORPHYRIN MACROCYCLES, (2014).

[6] M. Jugovac, A. Cossaro, A. Verdini, L. Floreano, D. Lüftner, P. Puschnig, V. Feyer, C.M. Schneider, On-surface nickel porphyrin mimics the reactive center of an enzyme cofactor, Chem. Commun. (2018).

[7] H.D. Pranowo, F. Mulya, H.A. Aziz, G.A. Santoso, Study of substituent effect on properties of Platinum (II) porphyrin semiconductor using density functional theory, Indones. J. Chem. 18 (2018) 742–748.

[8] M. Cao, A. Gao, Y. Liu, Y. Zhou, Z. Sun, Y. Li, F. He, L. Li, L. Mo, R. Liu, Theoretical study on electronic structural properties of catalytically reactive metalloporphyrin intermediates,

Catalysts. 10 (2020) 224.

[9] D.K. Deda, B.A. Iglesias, E. Alves, K. Araki, C.R.S. Garcia, Porphyrin derivative nanoformulations for therapy and antiparasitic agents, Molecules. 25 (2020) 2080.

[10] J.M. Gallego, Macrocycle metalation on solid surfaces, (2018).

[11] R. Chen, Y. Wang, Y. Ma, A. Mal, X.-Y. Gao, L. Gao, L. Qiao, X.-B. Li, L.-Z. Wu, C. Wang, Rational design of isostructural 2D porphyrin-based covalent organic frameworks for tunable photocatalytic hydrogen evolution, Nat. Commun. 12 (2021) 1–9.

[12] C.-R. Zhang, L.-H. Han, J.-W. Zhe, N.-Z. Jin, Y.-L. Shen, J.-J. Gong, H.-M. Zhang, Y.-H. Chen, Z.-J. Liu, The role of terminal groups in electronic structures and related properties: The case of push–pull porphyrin dye sensitizers for solar cells, Comput. Theor. Chem. 1039 (2014) 62–70.

[13] F. Mulya, G.A. Santoso, H.A. Aziz, H.D. Pranowo, Design a better metalloporphyrin semiconductor: A theoretical studies on the effect of substituents and central ions, in: AIP Conf. Proc., AIP Publishing LLC, 2016: p. 80006.

[14] H.A. Aziz, G.A. Santoso, F. Mulya, H.D. Pranowo, Molecular and electronic structure of some symmetrically meso-substituted Hg (II)-porphyrin complexes, Asian J. Chem. 29 (2017) 2224–2226.

[15] A.S. Shalabi, M.M. Assem, K.A. Soliman, A.M. El Mahdy, H.O. Taha, Performance of metalloporphyrin malonic acids as dye sensitizers for use in dye-sensitized solar cells assessed by density functional theory, Mater. Sci. Semicond. Process. 26 (2014) 119–129.

[16] J. Barbee, A.E. Kuznetsov, Revealing substituent effects on the electronic structure and planarity of Ni-porphyrins, Comput. Theor. Chem. 981 (2012) 73–85.

[17] U. Utari, K. Kusumandari, B. Purnama, M. Mudasir, K. Abraha, Surface Morphology of Fe (III)-Porphyrin Thin Layers as Characterized by Atomic Force Microscopy, Indones. J. Chem. 16 (2016) 233–238.

[18] G. Harrach, Z. Valicsek, O. Horváth, Water-soluble silver (II) and gold (III) porphyrins: The effect of structural distortion on the photophysical and photochemical behavior, Inorg. Chem. Commun. 14 (2011) 1756–1761.

[19] W. Zheng, N. Shan, L. Yu, X. Wang, UV–visible, fluorescence and EPR properties of porphyrins and metalloporphyrins, Dye. Pigment. 77 (2008) 153–157.

[20] X.-F. Wang, J. Xiang, P. Wang, Y. Koyama, S. Yanagida, Y. Wada, K. Hamada, S. Sasaki, H. Tamiaki, Dye-sensitized solar cells using a chlorophyll a derivative as the sensitizer and carotenoids having different conjugation lengths as redox spacers, Chem. Phys. Lett. 408 (2005) 409–414.

[21] M.S. Seo, N.H. Kim, K.-B. Cho, J.E. So, S.K. Park, M. Clémancey, R. Garcia-Serres, J.-M. Latour, S. Shaik, W. Nam, A mononuclear nonheme iron (IV)-oxo complex which is more reactive than cytochrome P450 model compound I, Chem. Sci. 2 (2011) 1039–1045.

[22] J.W. Shin, S.R. Rowthu, M.Y. Hyun, Y.J. Song, C. Kim, B.G. Kim, K.S. Min, Monomeric, trimeric, and tetrameric transition metal complexes (Mn, Fe, Co) containing N, N-bis (2-pyridylmethyl)-2-aminoethanol/-ate: preparation, crystal structure, molecular magnetism and oxidation catalysis, Dalt. Trans. 40 (2011) 5762–5773.

[23] W. Liu, J.T. Groves, Manganese porphyrins catalyze selective C– H bond

halogenations, J. Am. Chem. Soc. 132 (2010) 12847–12849.

[24] M.M. Pereira, L.D. Dias, M.J.F. Calvete, Metalloporphyrins: bioinspired oxidation catalysts, Acs Catal. 8 (2018) 10784–10808.

[25] S. Yamazaki, Metalloporphyrins and related metallomacrocycles as electrocatalysts for use in polymer electrolyte fuel cells and water electrolyzers, Coord. Chem. Rev. 373 (2018) 148–166.

[26] G.-P. Yan, D. Bischa, S.E. Bottle, Synthesis and properties of novel porphyrin spin probes containing isoindoline nitroxides, Free Radic. Biol. Med. 43 (2007) 111–116.

[27] M.L. Jabbar, K.J. Kadhim, Linear & nonlinear optical properties of undoped & doped graphene nanoribbon via TD-DFT study, in: AIP Conf. Proc., AIP Publishing LLC, 2020: p. 30011.

[28] N.H. Al-Saadawy, Synthesis, Characterization and Theoretical Studies of New Organotellurium Compounds Based on (4-(((1S, E)-1, 7, 7-trimethylbicyclo [2.2. 1] heptan-2-ylidene) amino) phenyl) mercury (II) Chloride, Indones. J. Chem. (2021).

[29] M.L. Jabbar, Theoretical study for the interactions of Coronene-Y interactions by using Density functional theory with hybrid function, Univ. Thi-Qar J. 13 (2018) 28–41.

[30] A.D. Becke, Density-functional thermochemistry. II. The effect of the Perdew–Wang generalized-gradient correlation correction, J. Chem. Phys. 97 (1992) 9173–9177.

[31] M. H Muzel, A.S. Alwan, M.L. Jabbar, Electronical Properties for (CxHyZ2-NO) Nanoclusters, Curr. Nanomater. 2 (2017) 33–38.

[32] M.L. Jabbar, K.J. Kadhim, Electronic Properties of Doped Graphene Nanoribbon and the Electron Distribution Contours: A DFT Study, Russ. J. Phys. Chem. B. 15 (2021) 46–52.

[33] C. Lee, W. Yang, R.G. Parr, Development of the Colle-Salvetti correlation-energy formula into a functional of the electron density, Phys. Rev. B. 37 (1988) 785.

[34] A.S. Alwan, Density functional theory investigation of (C4H2N2) 3 nanocluster and (C4H2N2) 3--P, Al, As, B, C and in nanoclusters, in: AIP Conf. Proc., AIP Publishing LLC, 2020: p. 30013.

[35] M.L. Jabbar, Computational studies on electronic and optical properties of dopamine derivatives structure: A DFT study, J. Mech. Behav. Mater. 30 (2021) 279–284.

[36] N.M. O'boyle, A.L. Tenderholt, K.M. Langner, Cclib: a library for package-independent computational chemistry algorithms, J. Comput. Chem. 29 (2008) 839–845.

[37] M.L. Jabbar, Some electronical properties for Coronene-Y interactions by using density functional theory (DFT), J. Basrah Res. 44 (2018).

[38] A.S. Alwan, S.K. Ajeel, M.L. Jabbar, Theoretical study for Coronene and Coronene-Al, B, C, Ga, In and Coronene-O interactions by using Density Functional theory, Univesity Thi-Qar J. 14 (2019).

[39] V.P. Gupta, Principles and applications of quantum chemistry, Academic Press, 2015.

[40] R. Vivas-Reyes, A. Aria, Evaluation of group electronegativities and hardness (softness) of group 14 elements and containing functional groups through density functional theory and correlation with NMR spectra data, Eclética Química. 33 (2008) 69–76.

[41] Mj. Frisch, G. Trucks, H.B. e al Schlegel, G.E. Scuseria, M.A. Robb, J.R. Cheeseman, J.A. Montgomery Jr, T. Vreven, K.N. Kudin, J.C. Burant, Gaussian 03, revision C. 02, (2004).

[42] M.A. Omar, Elementary solid state physics: principles and applications, Pearson Education India, 1975.

[43] A.A. Abrikosov, Fundamentals of the Theory of Metals, Courier Dover Publications, 2017.

[44] T. Adachi, T. Sunada, Density of states in spectral geometry, Comment. Math. Helv. 68 (1993) 480–493.

[45] M.A. Ahmed, Z.M. Abou-Gamra, H.A.A. Medien, M.A. Hamza, Effect of porphyrin on photocatalytic activity of TiO2 nanoparticles toward Rhodamine B photodegradation, J. Photochem. Photobiol. B Biol. 176 (2017) 25–35.